



Accurate estimation of log MOE from non-destructive standing tree measurements

Chandan Kumar¹ · Steven Psaltis^{2,3} · Henri Bailleres¹ · Ian Turner^{2,3} · Loic Brancheriau⁴ · Gary Hopewell¹ · Elliot J. Carr² · Troy Farrell² · David J. Lee⁵

Received: 16 April 2020 / Accepted: 11 January 2021 / Published online: 22 January 2021
© INRAE and Springer-Verlag France SAS, part of Springer Nature 2021

Abstract

• **Key message** A novel non-destructive method has been developed to predict modulus of elasticity (MOE) of logs using measurements taken from cores extracted from discs. The trees were felled and cut into logs to allow validation of our method; however, similar results would be obtained if the cores were extracted from standing trees. The method shows that a single core from breast height is sufficient to predict MOE of logs, allowing early grading and sorting of logs for optimal use and processing.

• **Context** Early estimation of log MOE allows efficient sorting and grading of logs which can improve the financial return and reduce wastage of wood.

• **Aims** This work aims to predict the MOE of logs accurately from measurements taken on cores obtained from trees.

• **Methods** The MOE of the logs was predicted using ultrasound measurements conducted on small segments obtained from cores using two different approaches: segment average and integral average. Sixty-eight trees from locally developed F₁ and F₂ hybrid pines (slash pine × Caribbean pine hybrids, *Pinus elliottii* var. *elliottii* × *P. caribaea* var. *hondurensis* (PEE × PCH cross)) were felled and cut into logs to validate the results. The Beam Identification by Non-destructive Grading (BING) method was used to measure a reference dynamic MOE (BING-MOE) for each log, and this was compared with the estimated log MOE.

• **Results** Strong correlations ($r = 0.79$ to 0.91) between measured log MOE and estimated log MOE were obtained. This study revealed that a single core from the breast height (1.3 m) of a tree allows a good prediction of the log MOE. Tree height, spacing, and diameter had no significant effect on the log MOE prediction. The segment average MOE under predicts the BING-MOE, whereas the integral average method provides very little bias in the prediction. Furthermore, the prediction errors from the regression analysis for all logs were greater in the segment average method compared with the integral average method.

• **Conclusion** This paper presented a novel non-destructive evaluation method capable of predicting the MOE of the whole log by combining data available from a single breast-height core extracted from standing trees with our integral average MOE approach. The integral average method predicted the BING-MOE more accurately with lower bias compared with other existing tools without any complex equipment, analysis, and statistical calibration for segregating out individual trees or stands. The method can potentially be used to predict the log MOE of other tree species and extended to predict MOE of individual boards that can be sawn from a log.

Keywords Log MOE · Non-destructive · Prediction · Standing tree measurement · Core

Handling Editor: Jean-Michel Leban

✉ Chandan Kumar
chandan.kumar@daf.qld.gov.au

Extended author information available on the last page of the article

1 Introduction

The forest sector's prosperity is becoming less dependent on the traditional volume optimisation and more dependent on value optimisation (Todoroki and Rönqvist 2002). In order to extract the best value from the wood fibre, it is essential that the performance of the forest resource be

assessed as soon as possible along the wood value chain. Assessment of log stiffness properties and efficient sorting of logs can improve the financial return and reduce wastage of wood. For some processing sectors, such as the sawmilling industry or structural wood manufacturing industry, wood stiffness is the main factor driving forest value. The main product manufactured from many softwood resources is sawn timber in the form of standard board sizes. The value of these boards depends on its mechanical performances assessed using standard procedures. Non-structural and structural grades are specified based on product stiffness quantified by the modulus of elasticity (MOE) and its strength quantified by the modulus of rupture (MOR). The standard structural grade rating is often limited by its stiffness. The MOE dictates the mechanical grade of the board. A board's market value is directly linked to its grade based on individual grading performance, with structural grade boards worth $\geq \$350 / \text{m}^3$ and non-structural boards worth approximately $\$80 / \text{m}^3$ (Baillères et al. 2019). Moreover, stiffness measurements can also be used to improve breeding, planting, and silviculture management so that future forests have better properties (Legg and Bradley 2016a). This is critical for young, fast growing plantations, since the variation of the important wood properties is substantial within and between trees, even for trees of the same age and from the same stand (Huang et al. 2003; Zobel and Buijtenen 1989; Zobel and Jett 2012; Zobel and Sprague 2012). Therefore, accurate and early measurement of stiffness properties (modulus of elasticity, MOE) is essential to grade and sort logs allowing optimal use of wood resources.

During the past few decades, research has developed and refined non-destructive evaluation (NDE) approaches and tools for measuring the MOE of logs. As described by Schimleck et al. (2019), an approach can be defined as non-destructive if it is applied to either a standing tree or a felled log or if the method is used on a radial sample. The radial sample can be obtained from either an increment core or disc after felling. These authors discussed various NDE tools for assessing wood properties in both the field and laboratory including acoustics, Pildyn, Resistograph, Rigidimeter, computed tomography (CT) scanning, the Scion's DiscBot, near-infrared (NIR) spectroscopy, radial sample acoustics, and SilviScan. A tree bending apparatus (rigidimeter) was developed by several researchers to determine MOE of standing trees (Koizumi 1987; Koizumi and Ueda 1986; Mamdy et al. 1999; Prestemon and Buongiorno 2000). This method measured the deflection of the trunk at a specific point under a bending moment. The authors obtained a coefficient of determination of 0.54 between tree MOE and the average MOE of the dried boards cut from the same tree; however, this method was fairly time-consuming

as only 20–50 trees could be measured per day depending on the apparatus (Launay et al. 2000; Wessels et al. 2011). Launay et al. (2000) highlighted the possibility of measuring more than 50 trees a day with a team of three people under good weather conditions.

Acoustic techniques are the most commonly and commercially used techniques and are inexpensive, fast, robust, and easily used in the field. Acoustic tools have been used to assess standing trees before harvest, enabling management, planning, harvesting, and wood processing to be carried out in a way that maximises extracted value from the resource (Schimleck et al. 2019). These methods measure stress wave speed through the stem, generated by tapping one end with a light hammer. The time of flight (TOF) of the acoustic wave is measured between the transmitter probe and receiver probe (Wang and Ross 2002; Wessels et al. 2011). The wave speed and a dynamic MOE are calculated from the TOF and density. Usually, for a given tree type, a fixed density is assumed to calculate MOE. For example, the green density of radiata pine is often chosen to be approximately 1050 kg/m^3 (Legg and Bradley 2016a). Acoustic measurement techniques based on the above density assumptions have been applied to segregate forest products by measuring a stiffness on standing trees, felled logs, and sawn timber (Legg and Bradley 2016a; Wang and Ross 2002). The coefficient of determination between standing tree acoustic measures and the static modulus of elasticity (MOE_s) of defect-containing timber from these trees varied from 0.33 to 0.64 depending on the nature of the resources and the variation amplitude of the MOE (Ikeda 2002; Ishiguri et al. 2006; Matheson et al. 2002). In studies relating dynamic MOE (MOE_d) of standing trees with MOE_s and modulus of rupture (MOR) of clear pieces of wood from those trees, it was found that correlation coefficients of 0.63 to 0.69 for MOE_s and 0.36 to 0.65 for MOR were obtained (Wang et al. 2000, 2007b; Wessels et al. 2011). However, the constant density assumption often leads to large measurement approximation errors since the actual average density of the tree stems may vary significantly along the radius of the stem due to variations across the growth rings. This velocity measurement technique therefore has a potential source of error since the MOE is proportional to the square of the velocity. Moreover, the simplified equation used to calculate MOE using the acoustic method assumes that the vibration is in an isotropic, homogeneous and infinite continuous media (Strutt and Rayleigh 1945). The TOF acoustic tool can provide biased results in older stands as outerwood properties become more consistent in older trees. An alternative acoustic approach, i.e. resonance methods, was also used for felled logs, and the measurement principles for TOF and resonance applied

to standing trees and logs are different (Auty and Achim 2008; Wang et al. 2007a). Resonance approaches are more representative of a whole log and considered more accurate than TOF methods (Simic et al. 2019).

Pilodyn is one of the least invasive tools and involves the injection of a sticker pin (spring-loaded) with a known force. The penetration depth is negatively correlated with wood density. However, the accuracy of Pilodyn is limited (Cown 1978) and considered unreliable for tree selection in breeding programs (Raymond et al. 1998). Moreover, the Pilodyn tools evaluate only the outermost rings of the wood, and thus, a stem's mean density is not representative (Gao et al. 2017).

The Resistograph has been used historically to identify decay and other defects in trees and poles. It provides a rapid and less expensive means of collecting wood density data. Research has shown that the IML PD400 (Resi) can explain over 80% of the variance in the average density data (Downes and Lausberg 2016; Downes et al. 2018). However, there are issues regarding drag, wear of the Resi needle, the effect of moisture on the resistance values, and the tendency of the needle to curve right or left (Schimleck et al. 2019).

Internal MOE variation analysis has been measured on increment cores (Giroud et al. 2017; Hong et al. 2015; Ivković et al. 2008). The MOE of wood varies significantly along the radius within a tree (Baillères et al. 2019; Zobel and Buijtenen 1989) compared with its tangential or longitudinal variation. Bucur (1983) determined stiffness and shear moduli of 5-mm diameter increment core using an ultrasonic velocity method and found good correlation between the ultrasound method and static bedding test. The ultrasonic method is capable of rapidly detecting the differences between individual characteristics of living trees.

SilviScan™ predicts the MOE by measuring wood density and microfibril angle using an X-ray densitometer and X-ray diffractometer respectively, from increment cores taken from trees (Evans et al. 2000). This measurement method is not cost-effective as it requires a large investment and has high running costs. Nevertheless, it provides a very localised (less than 0.5 mm) measurement of the stiffness along the radius (Knowles et al. 2004).

Near-infrared (NIR) spectroscopy can be applied to analyse samples obtained from increment cores. The analysis involves a calibration process through a chemometric approach using training samples (calibration set) to develop the mathematical relationship between the NIR spectra and the property of interest (Wessels et al. 2011). Schimleck et al. (2001) obtained

coefficients of determination of 0.90 and 0.77 for the relationship between NIR data and MOE and MOR, respectively, for clear *Eucalyptis delegatensis* samples of the calibration set. Thumm and Meder (2001) used NIR to predict MOE of clear wood specimens of radiata pine (*Pinus radiata* D. Don). The model was calibrated on NIR spectra from 404 samples, and the model was then able to predict the stiffness of 80 test samples with 14% error. Kelley et al. (2004) measured NIR spectra and mechanical properties of 1000 small clear wood sample of six softwoods. The authors used a partial least squares (PLS) approach to predict mechanical properties and NIR spectra and obtained R^2 values greater than 0.85. Further studies have also found higher values of R^2 for MOE (Gindl et al. 2001; Via et al. 2003). However, Via et al. (2003) found that the predictability of the model decreased significantly when pith wood was considered. Similar decreased predictability was observed for full-sized defect-containing timber (Hoffmeyer and Pedersen 1995) and compression wood (Gindl et al. 2001). In summary, NIR spectroscopy is able to predict many basic properties; however, this approach requires a robust calibration and ongoing recalibration. The relationship developed through calibration (training data) is used to predict measurement of unknown samples.

The overall MOE of a stem and tree also depends on the variation or pattern of internal MOE variation. Therefore, consideration of internal variation in predicting the stem/tree MOE should improve the prediction capability. Although increment cores are able to provide detailed information on the variation of properties within the tree, the results obtained from increment coring have not been used to predict the MOE of logs.

In this work, we investigate the use of MOE measurements taken on cores from trees to predict log MOE of locally developed F_1 and F_2 hybrid pines (slash pine \times Caribbean pine hybrids, *Pinus elliottii* var. *elliottii* \times *P. caribaea* var. *hondurensis* (PEE \times PCH cross)). These cores were cut into 20 mm segments on which measurements were made. This allows us to account for the large internal pith-to-bark variation that is observed in MOE when formulating these predictions. We use an approach based on an asymmetric sigmoid function to model the MOE variation with radius. To calculate the MOE of a log, we integrate this function over the cross-sectional area to account for the varying contribution to the average based on the area of timber. This is contrasted to taking a simple arithmetic average of the core segments, where each segment's MOE would be weighted equally. In the remainder of this article we refer to the following types of MOE:

1. BING-MOE: the reference measurement made on the logs using the BING method.
2. US-MOE: the measurement made on core segments using the ultrasound technique.
3. US-MOE_{SEG}: the estimated log US-MOE obtained from the segment average.
4. US-MOE_{SPL}: the estimated log US-MOE obtained from the integral average of a 5-parameter logistic function.

Each of these will be discussed further below.

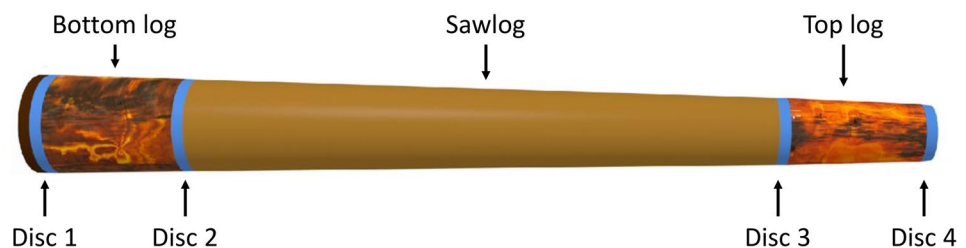
2 Material and methods

2.1 Overall approach

Southern pine samples were stratified and collected from southeast Queensland (SEQ) plantation forests. A total of 68 trees of 19, 24 and 28 years of age were harvested from plantations in Beerburrum (latitude – 26.98 and longitude 152.98), Tuan (latitude – 25.79 and longitude 152.91), and Toolara (latitude – 25.98 and longitude 152.88) in SEQ.

The trees sampled for this study were a combination of locally developed F₁ and F₂ hybrid pines (slash pine × Caribbean pine hybrids, *Pinus elliottii* var. *elliottii* × *P. caribaea* var. *hondurensis* PEE × PCH cross): 30 trees from Tuan of 28 years of age were F₂ hybrid pine (a second filial hybrid of PEE × PCH cross), with stocking of 388 stems per hectare; 30 trees from Beerburrum of 19 years of age were F₁ hybrid pine (a first filial hybrid of PEE × PCH cross) with stocking between 200 and 1000 stems per hectare, and 8 trees from Toolara of 24 years of age were F₁ hybrid pine with stocking between 1006 and 2660 stems per hectare (Kumar et al. 2020). Trees at each location were collected using a stratified sampling system to ensure all harvestable diameter classes were sampled. The trees were cut to obtain a whole log which was subsequently cut into two small logs (1.2 m) from its top and bottom, one sawlog (3.9 m) from the middle, and four discs as shown in Fig. 1. The four discs are taken at approximately 0.92 m, 2.34 m, 6.46 m, and 7.88 m from the ground.

Fig. 1 Sacrificial sampling template showing the whole log, and three smaller logs and four discs sampled from the tree



All the logs (whole log, top log, sawlog, bottom log) were weighed and measured for BING-MOE using an acoustic resonance technique (discussed in Sect. 3.2) which was the experimental reference MOE used in this study. Four transverse cores cut out of the disc were segmented into 20-mm sections, conditioned at 12% moisture content, and their properties were measured using an ultrasound system (discussed in Sect. 3.4.1). These transverse cores represent the increment cores from standing trees. The US-MOE of the segments was used to estimate the MOE of the logs using two methods: (a) segment average MOE (US-MOE_{SEG}) and (b) integral average MOE (US-MOE_{SPL}, described in Sect. 3.3.2). The estimated (US-MOE_{SEG} and US-MOE_{SPL}) and experimental log MOE (BING-MOE) were then compared and analysed.

2.2 Experimental reference MOE (BING-MOE) by acoustic resonance technique

The MOE of each log was measured using Beam Identification by Non-destructive Grading (BING) (Paradis et al. 2017), which is a resonance acoustic method for estimating MOE. It consists of a microphone, an acquisition card (Pico Technology), two elastic supports, and a hand-held hammer (Baillères et al. 2009; Brancheriau 2014; Faydi et al. 2017).

For longitudinal vibrations, the following equation was used to determine the axial modulus of elasticity:

$$\text{BING - MOE} = 4L^2\rho\left(\frac{f_n}{n}\right)^2 \quad (1)$$

Here, L is the length of the beam (m), ρ is the density (kg/m³), and f_n is the vibration frequency of rank n (1/s).

This equation is valid for slender beams ($L/h \geq 10$, where h is the height of the beam) and only for the fundamental frequency (Brancheriau and Baillères 2002).

2.3 Correlation matrices, statistical analysis, and regression analysis

The correlation matrices, statistical analysis, and regression analysis were carried out using the open-source statistical package, R (RStudio Team 2015). The Spearman's

correlation coefficients between log BING-MOE (whole log, bottom log, sawlog, and top log) and other variables, namely, stocking, diameters, diameter at breast height (DBH), and height of the trees Pearson's correlation between MOE, were presented, and correlation with $p > 0.05$ are considered statistically insignificant and are left blank. For the regression analysis, the red line and red text in the figures show the regression line and coefficient when fitted with a zero intercept (regression through the origin), and blue colour represents ordinary regression with intercept.

2.4 Estimation of log MOE

The MOE of all three logs were estimated using two methods: segment average MOE and integral average MOE as discussed below.

2.4.1 Segment average MOE (US-MOE_{SEG})

Four transverse cores were cut out of the four discs, i.e., one core per disc. The cores were marked out at 20-mm intervals starting at the outer end (bark side) and a unique number marked on each segment towards the pith then from the other bark side towards the pith (see Fig. 2a and c). The segment markings and their relative position from the piths were marked on tracing paper as shown in Fig. 2b. The tracing papers were scanned, and the scanned images were cropped, and centroids of the rings, segments, and pith markings were identified using MATLAB® (MATLAB 2017). Then, the mean distances of the segments from the pith and the ring locations were calculated.

After mapping, the cores were segmented into 20-mm sections using a guillotine for further measurement (Fig. 2c). The unique identifier of each segment was used to maintain

Fig. 2 An example of a (a) whole core scan, (b) tracings of pith, cambial rings and segments, and (c) segments for Ultrasound MOE (US-MOE) measurement

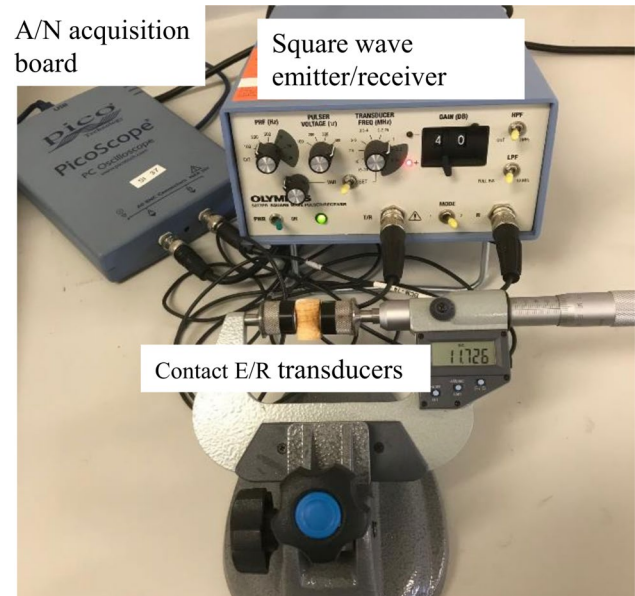
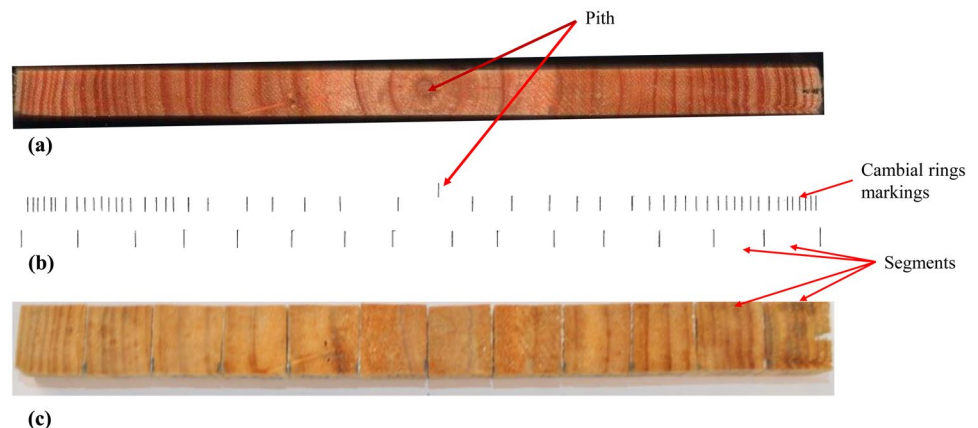


Fig. 3 Ultrasound apparatus for calculation of wood stiffness properties (US-MOE)

traceability to its original core, tree, plot, and compartment and logging area.

The mean wood stiffness value for each segment was determined using an ultrasound device (Fig. 3). We refer to the stiffness measured using this method as the ultrasound MOE (US-MOE). Each segment was placed between two transducers, and the segment's thickness was recorded. Measurements were performed in transmission mode at 1 MHz with a dry coupling (thin elastomer). The device ensured a constant, light contact pressure. The output signal was digitised to calculate the propagation time. The equipment used for this study shown in Fig. 3 included a PicoScope oscilloscope (Pico 3224), Olympus 5077PR square

wave emitter/receiver, two contact transducers (V103 Videscan, Olympus), and a computer.

The stiffness of each segment, expressed as US-MOE in megapascals (MPa), was determined through a corrective formula of the conventional equation (Rakotovololonalimanana et al. 2015):

where ρ = density (kg/m^3), V = wave velocity (m/s), L = segment thickness (m), and τ = propagation time (s).

$$\text{US - MOE} = \rho V^2 = \rho \left(\frac{L}{\tau} \right)^2, \quad (2)$$

To calculate the US-MOE_{SEG} of a log, the arithmetic mean of the US-MOE of the segments from each core was computed. We then compared this with the BING-MOE measured on the logs. The calculation of the US-MOE_{5PL} will be discussed in the next section.

2.4.2 Integral average MOE (US-MOE_{5PL})

Five parameter logistic model fitting The variation of wood properties (MOE) along the radius (pith to bark) has been described by a sigmoidal function (S-shaped curve) by several researchers (Bailleres et al. 2005; Zobel and Buijtenen 1989). In this study, a five-parameter logistic (5PL) function was used to describe the radial variation of US-MOE obtained from segment data. The 5PL model is widely used in biological literature (Ricketts and Head 1999; Wild 2013) and exhibits rapid initial growth (increase) before approaching a plateau and can incorporate asymmetry. The 5PL can dramatically improve the accuracy over the use of curves symmetric about their inflection point such as the four-parameter logistic (4PL) function (Gottschalk and Dunn 2005; Wild 2013). For our data, the 5PL function gave a root-mean-square error (RMSE) approximately 10% lower than the symmetric 4PL function. It is commonly shown that wood properties such as density and MOE follow this type of pattern, due to normal plant physiology and wood formation processes. The 5PL model used in this study for MOE is given by

$$m(r) = A + \frac{B - A}{\left(1 + \left(\frac{r}{C} \right)^D \right)^E}. \quad (3)$$

Here, r (m) is the radial position for the segment from the pith, A is the asymptotic maximum, B is the asymptotic minimum, C is the inflection point midway between A and B (when $E = 1$), D is the slope factor which characterises the steepness of the curve, and E is the asymmetry factor.

We have utilised an orthogonal distance regression (ODR) algorithm (Nocedal and Wright 2006) to obtain the best fit of the 5PL function to the measured data. ODR is

preferred over standard regression techniques when there may be an error in both the measured property and error in the independent variable (radial position in this case) (Boggs and Rogers 1990). The radial position corresponding to the US-MOE for each core segment was taken at the geometric centre of the segment. However, there may be errors associated with measuring this radial position due to the manual measurement, and it may not accurately reflect the true radial position for the measured value of US-MOE due to the different proportions of each tree ring in the segment. We have utilised MATLAB®'s constrained minimisation functions (MATLAB Optimization Toolbox 2016a) to implement orthogonal regression. To compare our orthogonal regression approach, we also performed fitting of the 5PL function using classical (ordinary) regression, which minimises the vertical distance between the data and the curve.

Calculation of US-MOE_{5PL} This section describes the methods applied to extract quantitative characteristic values such as the quantity of wood for a given level of performance (e.g., above 10,000 MPa) or the average MOE for a given age interval. The 5PL functions ($m(r)$) developed in the previous section were used to calculate the US-MOE_{5PL} of the logs. The US-MOE_{5PL} of a log section can be calculated using a single core and by applying the mean value theorem, where we assume that the log can be considered cylindrical. The mean value theorem gives that

$$\text{US - MOE}_{5\text{PL}} = \frac{1}{h\pi R^2} \int_0^h \int_0^{2\pi} \int_0^R m(r) r dr d\theta dz \quad (4)$$

where $m(r)$ is the MOE at radial coordinate r given by the fitted 5PL curve, θ is the standard polar angular coordinate, z is the axial coordinate, h is the length of the log, and R is the outer log radius. By assuming variation in the angular and longitudinal direction is negligible, we can reduce Eq. (4) to

$$\text{US - MOE}_{5\text{PL}} = \frac{2}{R^2} \int_0^R m(r) r dr. \quad (5)$$

We have used MATLAB® to calculate this integral. The value obtained by this method, defined here as the US-MOE_{5PL}, was directly compared with the BING-MOE.

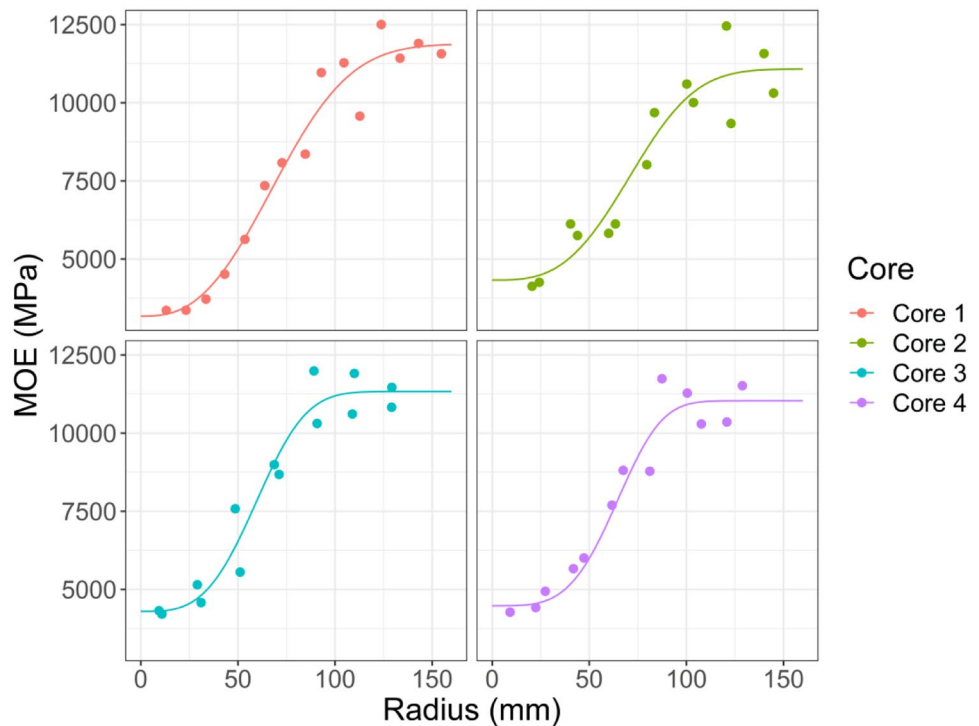
3 Results

3.1 5PL fitting results

Representative examples of the 5-parameter logistic (5PL) function fitted to the US-MOE of the segments against radius for four cores along the height of a tree are shown in Fig. 4.

Figure 5 shows a comparison between the root-mean-squared-error (RMSE) for orthogonal and ordinary regression. We see that orthogonal regression has an RMSE

Fig. 4 Example of 5PL fitting between US-MOE and radius of four cores taken from the bottom to the top of a log



consistently less than that for ordinary regression, thus justifying the use of this approach here.

3.2 Correlations between the variables and BING-MOE of the logs

As expected, a moderate negative correlation ($r = -0.76$ to -0.68) was found between stocking and diameters for all logs. Height of the trees showed a moderate positive correlation with all log BING-MOE as shown in

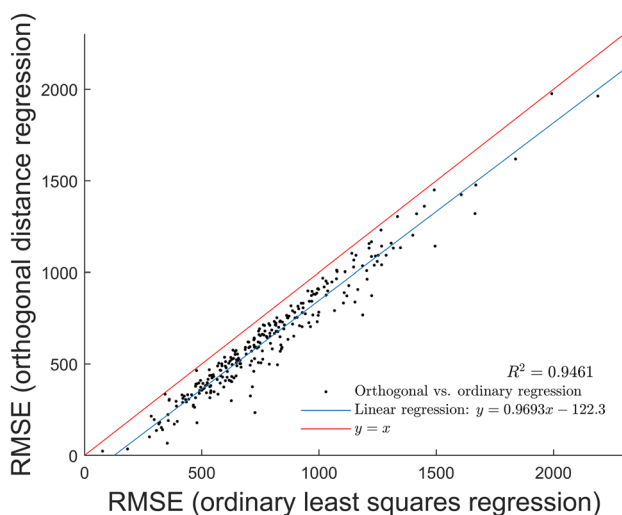


Fig. 5 Comparison between orthogonal and ordinary regression. Orthogonal regression consistently shows a lower RMSE when compared with ordinary regression

Fig. 6. A very strong correlation ($r = 0.89$ to 0.93) between BING-MOE of the logs from different heights and the whole log BING-MOE was found.

3.3 Correlations between BING-MOE and US-MOE_{SEG}

The BING-MOE for all logs were correlated with the US-MOE_{SEG} obtained from four cores. Overall, strong correlations (0.79 to 0.95) between whole log BING-MOE and US-MOE_{SEG} were found (Fig. 7).

The butt log BING-MOE was well correlated with US-MOE_{SEG} of cores 1, 2, and 3 having an r value of 0.89, 0.89, and 0.88 respectively, and slightly less correlated with the US-MOE_{SEG} at core height 4 ($r = 0.82$) (as shown in Fig. 7). US-MOE_{SEG} of cores 2 and 3 showed a better correlation for butt log, sawlog, and top log BING-MOE than whole log BING-MOE. The lowest correlation coefficients (0.79 to 0.85) were obtained between US-MOE_{SEG} for core 4 and BING-MOE (Fig. 7).

Figure 8 shows the linear regression between the BING-MOE of the logs and the US-MOE_{SEG} using core 1. The red line and red text in the figures show the regression line and coefficient when fitted with a zero intercept (regression through the origin), and blue colour represents ordinary regression with intercept. Overall, the results from Fig. 8 indicate that core 1 (i.e., the core was taken from the breast height of a tree) is sufficient to provide a reasonable prediction of log BING-MOE (with $R^2 = 0.64$ to 0.79). The RMSE values for the regression analysis between US-MOE_{SEG} from core 1 and BING-MOE were 1252, 1119,

Fig. 6 Correlation matrix of BING-MOE with height, diameter, and stockings

	Height	BING – MOE (butt log)	BING – MOE (sawlog)	BING – MOE (whole log)	BING – MOE (top log)	DBH	Top log diameter	Butt log diameter	Sawlog diameter	Whole log density	Sawlog density	Butt log density	Top log density
Stocking		+0.35		+0.28	+0.3	-0.76	-0.72	-0.74	-0.68				-0.36
Height		+0.5	+0.55	+0.57	+0.63	+0.31	+0.41	+0.36	+0.44		+0.4	+0.25	
BING – MOE (butt log)			+0.91	+0.9	+0.89	-0.26					+0.28	+0.38	
BING – MOE (sawlog)				+0.93	+0.92						+0.33	+0.36	
BING – MOE (whole log)					+0.93						+0.25	+0.34	
BING – MOE (top log)											+0.31	+0.41	
DBH						+0.9	+0.92	+0.9			+0.36		+0.49
Top log diameter							+0.98	+0.98			+0.42		+0.49
Butt log diameter								+0.98			+0.44		+0.52
Sawlog diameter									+0.98		+0.46		+0.54
Whole log density										+0.98	+0.34	+0.47	+0.35
Sawlog density												+0.58	+0.58
Butt log density													+0.62

1273, and 1165 MPa for whole log, butt log, sawlog, and top log respectively.

1 and BING-MOE were 1203, 1091, 1225, and 1027 MPa for whole log, butt log, sawlog, and top log respectively.

3.4 Correlations between BING-MOE and US-MOE_{5PL}

Figure 9 shows the correlation matrix between the BING-MOE and the predicted US-MOE_{5PL} using four cores. Similar to the US-MOE_{SEG}, the correlation coefficient, *r*, varies from 0.79 to 0.95. Figure 9 also shows that using the core at the top of the log gives lower prediction capabilities of the whole log, sawlog, and butt log (*r* = 0.80, 0.84, 0.79).

Figure 10 shows the regression analysis between the BING-MOE and US-MOE_{5PL} using core 1. In contrast to the US-MOE_{SEG} correlations shown in Fig. 8, significant improvement in prediction capability was obtained as the slope of the regression line with an intercept at zero (red line) is close to unity (shown in Fig. 10). The RMSEs for the linear regression model between the US-MOE_{5PL} of core

4 Discussion

The 5PL function was able to capture the overall trends exhibited in the data and acts to smooth the observed variation in US-MOE, particularly near the bark (Fig. 4). Therefore, the sigmoidal shape provides an effective US-MOE trajectory inside a tree which is supported by Zobel and Buijtenen (1989) and Bailleres et al. (2005). The 5PL model showed a large radial variation of US-MOE within a tree, which was similarly reported by Zobel and Buijtenen (1989).

As expected, a relative strong negative correlation (*r* = -0.76 to -0.68) was found between stocking and diameters for all logs. This is expected because the trees at higher stocking (i.e. closer spacing) have more competition thus

Fig. 7 Correlation matrix for the BING-MOE and US-MOE_{SEG} from four cores

	BING – MOE (butt log)	BING – MOE (sawlog)	BING – MOE (top log)	US – MOE _{SEG} (core 1)	US – MOE _{SEG} (core 2)	US – MOE _{SEG} (core 3)	US – MOE _{SEG} (core 4)
BING – MOE (whole log)	+0.91	+0.95	+0.94	+0.8	+0.85	+0.83	+0.79
BING – MOE (butt log)		+0.91	+0.92	+0.89	+0.89	+0.88	+0.82
BING – MOE (sawlog)			+0.92	+0.8	+0.88	+0.86	+0.81
BING – MOE (top log)				+0.86	+0.89	+0.89	+0.85
US – MOE _{SEG} (core 1)					+0.9	+0.89	+0.86
US – MOE _{SEG} (core 2)						+0.91	+0.89
US – MOE _{SEG} (core 3)							+0.91

slower growth rates and smaller diameters. The correlation coefficient (r) between density and BING-MOE of the corresponding log was weak with a value of 0.20, 0.38, 0.33, and 0.20 for whole log, butt log, sawlog, and top log respectively. Butler et al. (2017) and Knowles et al. (2004) also reported a similar weak correlation between basic density and mean lumber MOE. The correlation between MOE and density of logs becomes weaker for the relatively upper logs of the tree possibly because of less variation in density near the top of the tree as the juvenile wood proportion increase with height.

Correlations between BING-MOE and US-MOE_{SEG} (Fig. 7) indicate that the US-MOE_{SEG} can explain 62 to 89% of the variance in log BING-MOE. Core 4 provided the lowest correlation coefficients between US-MOE_{SEG} and BING-MOE (0.79 to 0.85), likely due to core 4 being the topmost core with a smaller diameter, thus providing fewer segments compared with the bottom core (core 1). Similar results were found for the US-MOE_{5PL} using core 4 and BING-MOE of the logs (Fig. 9). The segment sampling methodology that cuts the segments sequentially from the bark to the pith may explain this tendency. Often the segment close to the pith

could not be measured because of defects, or because they were undersize (< 20 mm). Therefore, the segments with lower US-MOE measurements were less represented when the reconstruction method was applied on small cores from the top of the whole log. Consequently, the higher US-MOE segments (outer segments) have greater weighting and could explain the overestimation on the smaller cores. Moreover, the top core (core 4) contains wood formed in the later years and does not represent the wood formed during early growth of the tree. Thus, core 4 may result in a less accurate representation of actual log BING-MOE.

The coefficient of determination (R^2) between the US-MOE_{SEG} using core 1 i.e. the breast height core (Fig. 8) and BING-MOE varies between 0.63 and 0.76. On the other hand, the correlation between BING-MOE and US-MOE_{5PL} using core 1 provided coefficient of determination (R^2) values of between 0.65 and 0.79. Therefore, a breast height core can explain 63–76% and 65–79% of BING-MOE of the logs obtained from various heights of the tree (top log, sawlog, and butt lot) by using segment average and integral average approach respectively. However, the most important difference between the two

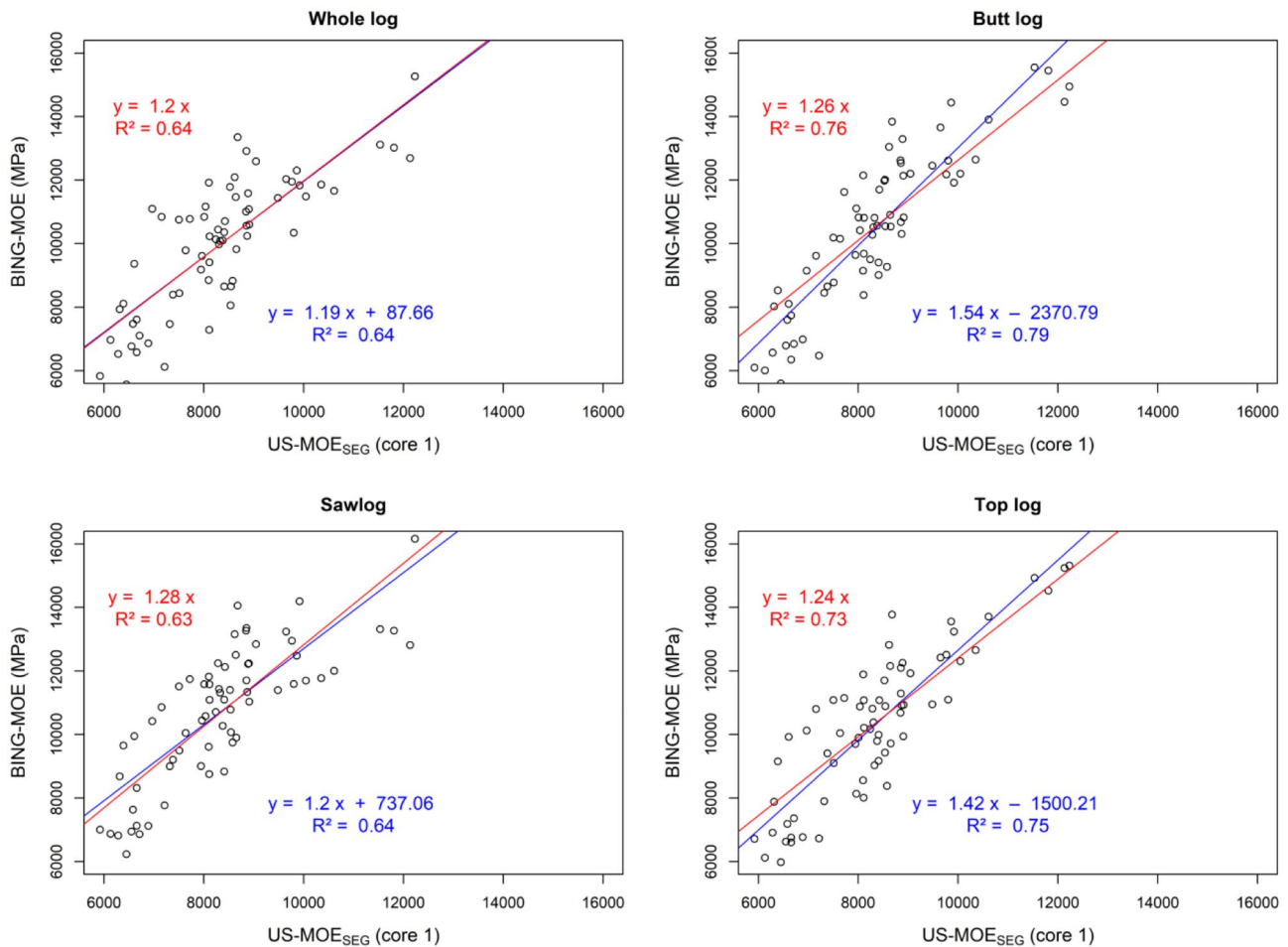


Fig. 8 Regression of BING-MOE and US-MOE_{SEG} from core 1

methods (i.e. segment average and integral average) is pointed out by the slopes of the regression line when fitted through the origin. The slope of the regression line with zero intercept for the segment average method is much higher (varies from 1.2 to 1.28 as shown in Fig. 8), compared with the same obtained from the integral average method (varies from 1.01 to 1.08 as shown in Fig. 10). This means the US-MOE_{SEG} under predicts the BING-MOE by 20–28%, whereas the US-MOE_{5PL} provides very small bias in the prediction of BING-MOE from a breast height core. Some other methods, such as acoustic velocity, over predict the MOE, and some corrections using density or moisture content can be applied to obtain an adjusted MOE and reduce bias in the prediction (Mora et al. 2009; Paradis et al. 2013). In contrast, the integral average method provides very minimal bias without any adjustment. This is possibly because the integral approach takes into account the amount (or area) of wood having a given US-MOE along the radius, whereas the segment average only takes the arithmetic

average US-MOE of the large variation along the radius, and hence, each radial position is assumed to contain the same amount of wood. This results in less bias between the measured and predicted MOE values. The RMSE values obtained from regression analysis for all logs were greater in the segment average method compared with the integral average method.

The integral average method provided much better prediction compared with existing tools with an R^2 up to 0.79. Knowles et al. (2004) reported $R^2 = 0.17$ and 0.50 for IML hammer (stress wave technique) and SilviScan-2 respectively, and $R^2 = 0.0$ for Pilodyn. Paradis et al. (2013) reported $R^2 = 0.41$ between observed MOE and MOE estimated as a function of acoustic velocity and tree diameter which is slightly lower than the values of 0.65 and 0.55 reported by Mora et al. (2009) and Liu (2011). In an evaluation of three NDE technologies, the ST300, IML PD400 Resistograph, and ultrasound MOE measured on cores taken at breast height, the 5PL model had the highest correlation ($R^2 = 0.78$) and least bias (Baillères

Fig. 9 Correlation matrix for BING-MOE and US-MOE_{5PL} from four cores

	BING – MOE (butt log)	BING – MOE (sawlog)	BING – MOE (top log)	US – MOE _{5PL} (core 1)	US – MOE _{5PL} (core 2)	US – MOE _{5PL} (core 3)	US – MOE _{5PL} (core 4)
BING – MOE (whole log)	+0.91	+0.95	+0.94	+0.82	+0.85	+0.83	+0.8
BING – MOE (butt log)		+0.91	+0.92	+0.89	+0.9	+0.87	+0.84
BING – MOE (sawlog)			+0.92	+0.81	+0.87	+0.84	+0.79
BING – MOE (top log)				+0.9	+0.91	+0.88	+0.85
US – MOE _{5PL} (core 1)					+0.93	+0.88	+0.89
US – MOE _{5PL} (core 2)						+0.87	+0.88
US – MOE _{5PL} (core 3)							+0.91

et al. 2019). In addition, the ST300 over predicts log MOE measured using resonance acoustic systems (Legg and Bradley 2016b; Mora et al. 2009; Wang 2013). As the US-MOE_{5PL} system accurately measures internal variation in wood properties, the 5PL models can be extended with further mathematical modelling to predict MOE of individual boards can be sawn from a log. The major limitation of the US-MOE_{5PL} approach outlined here is the longer sample preparation and processing time compared with other methods such as Resistograph and ST300. Approximately 30–40 breast height cores per day can be collected for ultrasound screening and these need processing in the laboratory before the screening. In contrast, 160–200 ST300 readings can be collected and 300–400 Resistograph readings can be collected per day (Baillères et al. 2019; Schimleck et al. 2019). Another real advantage of the method presented in this article is that it does not rely on statistical calibration as required for the ST300 and Resistograph, so plantation coops that have trees with log MOE that are outside the range of those previously measured can be accurately predicted.

Moreover, since no statistical calibration is involved, the method and findings can also be applied to other tree species. The US-MOE_{5PL} technique also provides a relatively cheap way of estimating log MOE without any complex tools and analysis such as those needed for Silviscan and NIR. The method could be automated/labour cost could be minimised by developing a method for NIR measurement of the core to get the radial MOE profile and use the integral average method to predict log MOE.

When analysed together, the above results indicate that a single core from the bottom of the stem is sufficient to predict the log BING-MOE. The integral average method offers the advantage of non-destructive evaluation of logs by using a breast height core measurement from standing trees to evaluate and predict the MOE of the whole log with minimal bias. Moreover, mathematical manipulation to calculate the US-MOE_{5PL} is fairly simple and is not computationally intensive. Therefore we recommend the use of integral average method.

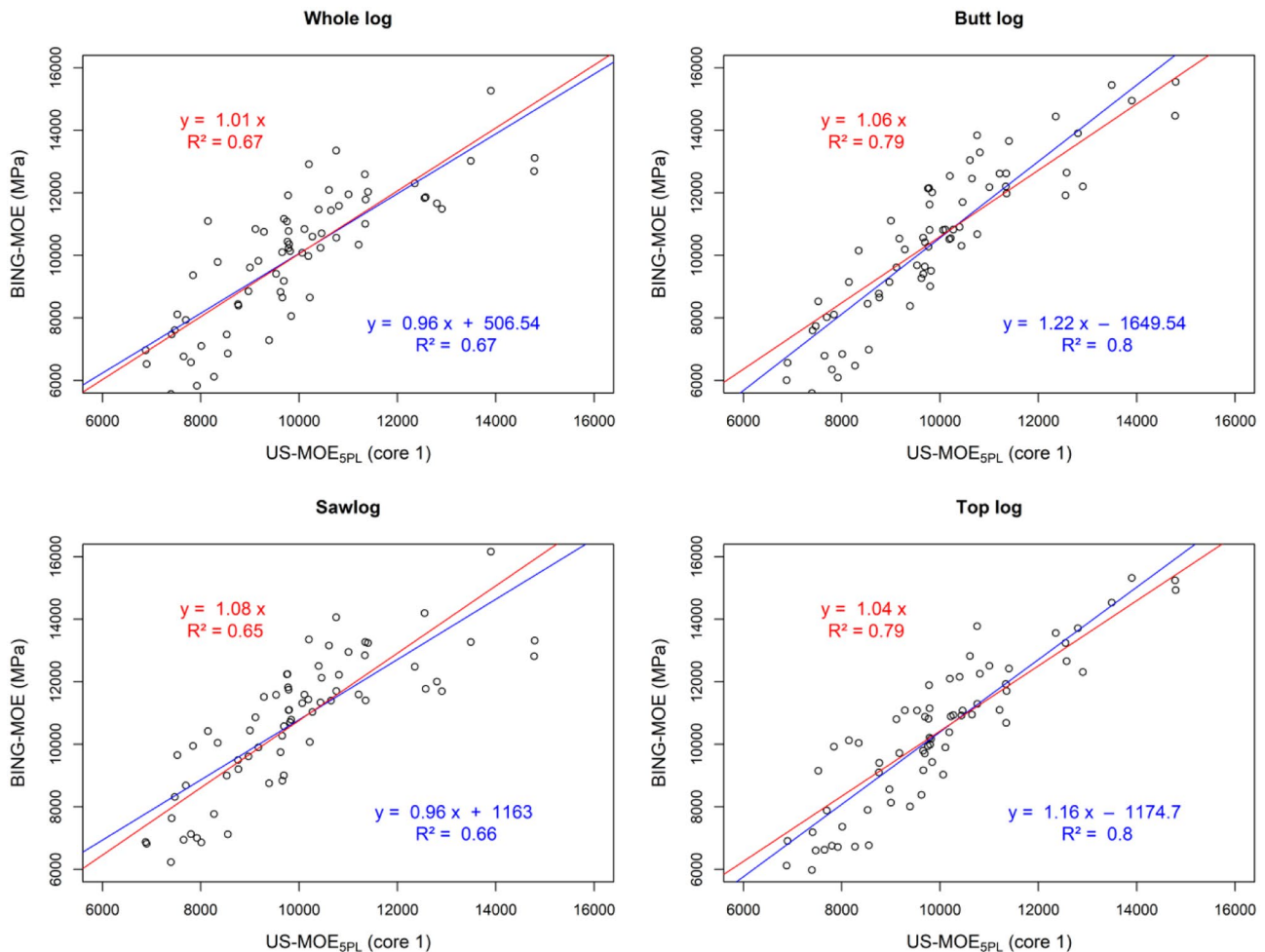


Fig. 10 Regression analysis for BING-MOE and US-MOE_{5PL} from core 1

5 Conclusion

The research reported here has demonstrated that increment coring can be successfully used to estimate the log MOE from a single breast height core. Moreover, the segments' US-MOE obtained from cores enabled the internal variation of MOE within a tree to be exhibited. The orthogonal regression analysis used to fit the 5PL function to the core US-MOE data provided lower RMSE values compared with ordinary regression. We found that stocking, diameter, height, and density showed a weak correlation with the log BING-MOE. Both the US-MOE_{SEG} and the US-MOE_{5PL} were well correlated with BING-MOE, having a correlation coefficient $r = 0.79$ to 0.95 . However, the integral average approach significantly improves the prediction capacity when regressed with BING-MOE because the slope of the regression line with a zero intercept was closer to unity compared with the higher values computed for the US-MOE_{SEG}. It was revealed that a single core at breast height was sufficient to predict the BING-MOE with a reasonable R^2 value. Therefore, a major

contribution of our work is that by combining data available from a single breast-height core extracted from standing trees with our US-MOE_{5PL} approach, we have identified a non-destructive evaluation method capable of predicting the MOE of the logs that can be cut from a tree. This non-destructive assessment of log MOE obtained from a breast height core can allow industry to sort logs allowing for optimal use of wood resources. The method described provided more accurate log MOE estimation with lower bias compared with other existing tools without any complex tools and analysis and statistical calibration. The method can potentially be used to predict the log MOE of other tree species and individual board MOE that can be sawn from a tree.

Acknowledgements This study was part of a project titled “Improving returns from Southern Pine plantations through innovative resource characterisation” Project PNC361-1415. We acknowledge the contribution by all staff at DAF Gympie and Salisbury Research Facility including Rhianna Robinson, Rica Minett, Jock Kennedy, John Huth, Chris Fitzgerald, Anton Zbonak, Cristina Latorre, Hernan Retamales, Eric Littee, William Leggate, Adam Redman, Tony Burrige, John

Oostenbrink, Kerri Chandra, and Tracey Menzies. The authors thank the anonymous reviewers and editors for their insightful comments that led to an improved final version of the manuscript.

Writing original draft, data analysis, methodology development, and conceptualisation: Chandan Kumar;

Orthogonal distance regression (ODR), mean value theorem, reviewing, and editing: Steven Psaltis, Ian Turner, Elliot J. Carr, Troy Farrell.

Supervision and conceptualisation: Henri Baillères,

Beam Identification by Non-destructive Grading (BING), review and editing: Loïc Brancheriau.

Sampling and experimental method development, review and editing: Gary Hopewell.

Sampling and experimental method development, review and editing, project management, funding acquisition: David J. Lee.

Funding The authors received financial support for the project from Forest and Wood Products Australia, DAF Forest Industries and industry partners: HQPlantations, Forest Corporation New South Wales, Hancock Victoria Plantations, and Hyne Timber Pty Ltd.


Data availability The datasets generated during and/or analysed during the current study are available in the University of the Sunshine Coast research data bank: <https://doi.org/10.25907/00001>.

References

- Auty D, Achim A (2008) The relationship between standing tree acoustic assessment and timber quality in Scots pine and the practical implications for assessing timber quality from naturally regenerated stands *Forestry* 81 <https://doi.org/10.1093/forestry/cpn015>
- Baillères H, Hopewell GP, Boughton G (2009) MOE and MOR assessment technologies for improving graded recovery of exotic pines in Australia *Forest & Wood Products Australia*, Project no: PNB040–0708
- Baillères H, Lee D, Kumar C, Psaltis S, Hopewell GP, Brancheriau L (2019) Improving returns from southern pine plantations through innovative resource characterisation, *Forest & Wood Products Australia*, Project no: PNC361–1415
- Baillères H, Vitrac O, Ramanantoandro T (2005) Assessment of continuous distribution of wood properties from a low number of samples: application to the variability of modulus of elasticity between trees and within a tree. *Holzforschung* 59:524–530
- Boggs PT, Rogers JE (1990) Orthogonal distance regression. *Contemporary Mathematics* 112:183–194
- Brancheriau L (2014) An alternative solution for the determination of elastic parameters in free-free flexural vibration of a Timoshenko beam. *Wood Sci Technol* 48:1269–1279. <https://doi.org/10.1007/s00226-014-0672-x>
- Brancheriau L, Baillères H (2002) Natural vibration analysis of clear wooden beams: a theoretical review. *Wood Sci Technol* 36:347–365
- Bucur V (1983) An ultrasonic method for measuring the elastic constants of wood increment cores bored from living trees. *Ultrasonics* 21:116–126. [https://doi.org/10.1016/0041-624X\(83\)90031-8](https://doi.org/10.1016/0041-624X(83)90031-8)
- Butler MA, Dahlen J, Eberhardt TL, Montes C, Antony F, Daniels RF (2017) Acoustic evaluation of loblolly pine tree- and lumber-length logs allows for segregation of lumber modulus of elasticity, not for modulus of rupture. *Ann For Sci* 74:20. <https://doi.org/10.1007/s13595-016-0615-9>
- Cown D (1978) Comparison of the Pilodyn and torsionmeter methods for the rapid assessment of wood density in living trees. *NZ J For Sci* 8:384–391
- Downes G, Lausberg M (2016) Evaluation of the RESI software tool for the prediction of HM200 within pine logs sourced from multiple sites across New Zealand and Australia *NZ. Solid Wood Innov* 15
- Downes G, Lausberg M, Potts B, Pilbeam D, Bird M, Bradshaw B (2018) Application of the IML Resistograph to the infield assessment of basic density in plantation eucalypts. *Aust For* 81:177–185
- Evans R, Ilic J, Matheson C (2000) Rapid estimation of solid wood stiffness using SilviScan. In: *Proceedings of 26th Forest Products Research Conference: Research developments and industrial applications and Wood Waste Forum*, Clayton, Victoria, Australia, 19–21 June 2000, CSIRO Forestry and Forest Products, pp 49–50
- Faydi Y, Brancheriau L, Pot G, Collet R (2017) Prediction of oak wood mechanical properties based on the statistical exploitation of vibrational response. *BioResources* 12:5913–5927
- Gao S, Wang X, Wiemann MC, Brashaw BK, Ross RJ, Wang L (2017) A critical analysis of methods for rapid and nondestructive determination of wood density in standing trees. *Ann For Sci* 74:27. <https://doi.org/10.1007/s13595-017-0623-4>
- Gindl W, Teischinger A, Schwanninger M, Hinterstoisser B (2001) The relationship between near infrared spectra of radial wood surfaces and wood mechanical properties. *J Near Infrared Spectrosc* 9:255–261
- Giroud G, Bégin J, Defo M, Ung C-H (2017) Regional variation in wood density and modulus of elasticity of Quebec's main boreal tree species. *For Ecol Manage* 400:289–299. <https://doi.org/10.1016/j.foreco.2017.06.019>
- Gottschalk PG, Dunn JR (2005) The five-parameter logistic: a characterization and comparison with the four-parameter logistic. *Anal Biochem* 343:54–65. <https://doi.org/10.1016/j.ab.2005.04.035>
- Hoffmeyer P, Pedersen J (1995) Evaluation of density and strength of Norway spruce wood by near infrared reflectance spectroscopy. *Holz als Roh-und werkstoff* 53:165–170
- Hong Z, Fries A, Wu HX (2015) Age trend of heritability, genetic correlation, and efficiency of early selection for wood quality traits in Scots pine. *Can J For Res* 45:817–825. <https://doi.org/10.1139/cjfr-2014-0465>
- Huang C-L, Lindström H, Nakada R, Ralston J (2003) Cell wall structure and wood properties determined by acoustics—a selective review. *Holz als Roh-und Werkstoff* 61:321–335
- Ikeda K (2002) Quality evaluation of standing trees by a stress-wave propagation method and its application. *Bulletin of the Shizuoka Prefecture Forestry Technology Center (Japan)*
- Ishiguri F, Kawashima M, Iizuka K, Yokota S, Yoshizawa N (2006) Relationship between stress-wave velocity of standing tree and wood quality in 27 Year Old Hinoki (*Chamaecyparis obtusa* Endl.) vol 55. <https://doi.org/10.2472/jsms.55.576>
- Ivković M, Gapare WJ, Abarquez A, Ilic J, Powell MB, Wu HX (2008) Prediction of wood stiffness, strength, and shrinkage in juvenile wood of radiata pine. *Wood Sci Technol* 43:237. <https://doi.org/10.1007/s00226-008-0232-3>
- Kelley SS, Rials TG, Groom LR, So C-L (2004) Use of near infrared spectroscopy to predict the mechanical properties of six softwoods. *Holzforschung* 58:252–260
- Knowles RL, Hansen LW, Wedding A, Downes G (2004) Evaluation of non-destructive methods for assessing stiffness of Douglas fir trees vol 34
- Koizumi A (1987) Studies on the estimation of the mechanical properties of standing trees by non-destructive bending test. *Research Bulletins of the College Experiment Forests-Hokkaido University (Japan)*

- Koizumi A, Ueda K (1986) Estimation of the mechanical properties of standing trees by bending tests. 1: test method to measure the stiffness of a tree trunk. *J Jpn Wood Res Soc (Japan)*
- Kumar C et al (2020) Data for the ultrasound estimation of log MOE from non-destructive standing tree measurements for the: 'Improving returns from southern pine plantations through innovative resource characterisation' project. University of the Sunshine Coast repository. V1. <https://doi.org/10.25907/00001>
- Launay J, Rozenberg P, Pâques LE, Dewitte JM (2000) A new experimental device for rapid measurement of the trunk equivalent modulus of elasticity on standing trees vol 57. <https://doi.org/10.1051/forest:2000126>
- Legg M, Bradley S (2016a) Measurement of stiffness of standing trees and felled logs using acoustics: a review. *J Acoust Soc Am* 139:588–604. <https://doi.org/10.1121/1.4940210>
- Legg M, Bradley S (2016b) Measurement of stiffness of standing trees and felled logs using acoustics: a review. *J Acoust Soc Am* 139. <https://doi.org/10.1121/1.4940210>
- Liu W (2011) Modelling color changes in wood during conventional drying. Université Laval
- Mamy C, Rozenberg P, Franc A, Launay J, Schermann N, Bastien J-C (1999) Genetic control of stiffness of standing Douglas fir; from the standing stem to the standardised wood sample, relationships between modulus of elasticity and wood density parameters. Part I *Ann For Sci* 56:133–143
- Matheson AC, Dickson RL, Spencer DJ, Joe B, Ilic J (2002) Acoustic segregation of *Pinus radiata* logs according to stiffness. *Ann For Sci* 59. <https://doi.org/10.1051/forest:2002031>
- MATLAB (2017) Version 9.6.0.1072779 (R2019a) Natick, Massachusetts: The MathWorks Inc
- MATLAB Optimization Toolbox (2016) The MathWorks. Natick, MA, USA
- Mora C, Schimleck L, Isik F, Mahon J, Clark A, Daniels R (2009) Relationships between acoustic variables and different measures of stiffness in standing *Pinus taeda* trees. *Can J For Res* 39:1421–1429. <https://doi.org/10.1139/X09-062>
- Nocedal J, Wright S (2006) Numerical optimization. Springer Science & Business Media
- Paradis N, Auty D, Carter P, Achim A (2013) Using a standing-tree acoustic tool to identify forest stands for the production of mechanically-graded lumber. *Sens* 13:3394–3408
- Paradis S, Brancheriau L, Baillères H (2017) Bing: Beam Identification by Non destructive Grading. <https://doi.org/10.18167/62696e67>
- Prestemon JP, Buongiorno J (2000) Determinants of tree quality and lumber value in natural uneven-aged southern pine stands. *Can J For Res* 30:211–219
- Rakotovololonimanana H, Chaix G, Brancheriau L, Ramamonjisoa L, Ramanantoandro T, Thevenon MF (2015) A novel method to correct for wood MOE ultrasonics and NIRS measurements on increment cores in *Liquidambar styraciflua* L. *Ann For Sci* 72:753–761. <https://doi.org/10.1007/s13595-015-0469-6>
- Raymond CA, Muneri A, MacDonald AC (1998) Non-destructive sampling for basic density in *Eucalyptus globulus* and *E. nitens*. *Appita J* 51:224–228
- Ricketts JH, Head GA (1999) A five-parameter logistic equation for investigating asymmetry of curvature in baroreflex studies *American Journal of Physiology-Regulatory, Integr Comp Physiol* 277:R441–R454
- RStudio Team (2015) RStudio: integrated development for R RStudio, Inc, Boston, MA
- Schimleck L et al (2019) Non-destructive evaluation techniques and what they tell us about wood property variation. For 10:728
- Schimleck L, Evans R, Ilic J (2001) Estimation of *Eucalyptus delegatensis* wood properties by near infrared spectroscopy. *Can J For Res* 31:1671–1675
- Simic K, Gendvilas V, O'Reilly C, Harte AM (2019) Predicting structural timber grade-determining properties using acoustic and density measurements on young Sitka spruce trees and logs. *Holzforschung* 73:139. <https://doi.org/10.1515/hf-2018-0073>
- Strutt JW, Rayleigh B (1945) The theory of sound. Dover
- Thumm A, Meder R (2001) Stiffness prediction of radiata pine clearwood test pieces using near infrared spectroscopy. *J Near Infrared Spectrosc* 9:117–122
- Todoroki C, Rönnqvist M (2002) Dynamic control of timber production at a sawmill with log sawing optimization. *Scand J For Res* 17:79–89. <https://doi.org/10.1080/028275802317221118>
- Via BK, Shupe TF, Groom LH, Stine M, So C-L (2003) Multivariate modelling of density, strength and stiffness from near infrared spectra for mature, juvenile and pith wood of longleaf pine (*Pinus palustris*). *J Near Infrared Spectrosc* 11:365–378
- Wang X (2013) Acoustic measurements on trees and logs: a review and analysis *Wood Science and Technology* 47. <https://doi.org/10.1007/s00226-013-0552-9>
- Wang X, Carter P, Ross R, Brashaw B (2007a) Acoustic assessment of wood quality of raw forest materials—a path to increased profitability. *For Prod J* 57:6–14
- Wang X, Ross RJ (2002) Nondestructive evaluation of green materials—recent research and development activities Nondestructive evaluation of wood Forest Products Society, Madison
- Wang X, Ross RJ, McClellan M, Barbour RJ, Erickson JR, Forsman JW, McGinnis GD (2000) Strength and stiffness assessment of standing trees using a nondestructive stress wave technique. United States Department of Agriculture, Forest Service, Forest Products Laboratory
- Wang X, Ross RJ, McClellan M, Barbour RJ, Erickson JR, Forsman JW, McGinnis GD (2007b) Nondestructive evaluation of standing trees with a stress wave method. *Wood Fiber Sci* 33:522–533
- Wessels CB, Malan FS, Rypstra T (2011) A review of measurement methods used on standing trees for the prediction of some mechanical properties of timber. *Eur J Forest Res* 130:881–893. <https://doi.org/10.1007/s10342-011-0484-6>
- Wild D (2013) The immunoassay handbook: theory and applications of ligand binding. Newnes, ELISA and related techniques
- Zobel BJ, Buijtenen JP (1989) Wood variation its causes and control. Springer series in wood science. Springer-Verlag New York Inc, New York, USA
- Zobel BJ, Jett JB (2012) Genetics of wood production. Springer Science & Business Media
- Zobel BJ, Sprague JR (2012) Juvenile wood in forest trees. Springer Science & Business Media

Authors and Affiliations

Chandan Kumar¹  · Steven Psaltis^{2,3} · Henri Bailleres¹ · Ian Turner^{2,3} · Loic Brancheriau⁴ · Gary Hopewell¹ · Elliot J. Carr² · Troy Farrell² · David J. Lee⁵

Steven Psaltis
steven.psaltis@qut.edu.au

Henri Bailleres
henri.bailleres@hyne.com.au

Ian Turner
i.turner@qut.edu.au

Loic Brancheriau
loic.brancheriau@cirad.fr

Gary Hopewell
Gary.Hopewell@daf.qld.gov.au

Elliot J. Carr
elliot.carr@qut.edu.au

Troy Farrell
t.farrell@qut.edu.au

David J. Lee
DLee@usc.edu.au

¹ Forest Product Innovation, Department of Agriculture and Fisheries, Queensland Government, Brisbane, Australia

² School of Mathematical Sciences, Queensland University of Technology, Brisbane, Australia

³ ARC Centre of Excellence for Mathematical and Statistical Frontiers, Queensland University of Technology, Brisbane, QLD 4000, Australia

⁴ CIRAD, Universite de Montpellier, 34398 Montpellier, France

⁵ Forest Industries Research Centre, University of the Sunshine Coast, Locked Bag 4, Maroochydore DC, QLD 4558, Australia